Chinese Chemical Letters 35 (2024) 109574

Contents lists available at ScienceDirect

Chinese Chemical Letters

journal homepage: www.elsevier.com/locate/cclet

Asymmetric macrocyclization enabled by Rh(III)-catalyzed C–H activation: Enantioenriched macrocyclic inhibitor of Zika virus infection

Chao Chen[a,b,c,g,1], Wenwen Yu[b,f,1], Guangen Huang[d,1], Xuelian Ren[e,1], Xiangli Chen[d], Yixin Li[a,f], Shenggui Liang[a,f], Mengmeng Xu[d], Mingyue Zheng[a,b], Yaxi Yang[a,b,c,f,*], He Huang[a,e,*], Wei Tang[d,e,*], Bing Zhou[a,b,c,d,f,g,*]

[a] School of Pharmaceutical Science and Technology, Hangzhou Institute for Advanced Study, University of Chinese Academy of Sciences, Hangzhou 310024, China
[b] State Key Laboratory of Drug Research, Shanghai Institute of Materia Medica, Chinese Academy of Sciences, Shanghai 201203, China
[c] Shandong Laboratory of Yantai Drug Discovery, Bohai Rim Advanced Research Institute for Drug Discovery, Yantai 264117, China
[d] School of Chinese Materia Medica, Nanjing University of Chinese Medicine, Nanjing 210023, China
[e] State Key Laboratory of Chemical Biology, Shanghai Institute of Materia Medica, Chinese Academy of Sciences, Shanghai 201203, China
[f] University of Chinese Academy of Sciences, Beijing 100049, China
[g] Department of Medicinal Chemistry, School of Pharmacy, Fudan University, Shanghai 201203, China

ARTICLE INFO

Article history:
Received 10 December 2023
Revised 24 January 2024
Accepted 26 January 2024
Available online 2 February 2024

Keywords:
C-H activation
Carboamidation
Enantioselective macrocyclization
Anti-Zika virus activity

ABSTRACT

The development of enantioselective C–H macrocyclizations to efficiently access structurally diversified macrocycles is highly desirable, but remain a big challenge. Herein, we reported the first rhodium(III)-catalyzed asymmetric intramolecular C–H macrocyclization, enabling the efficient synthesis of structurally diverse enantioenriched macrocycles. This robust enantioselective C–H macrocyclization has a broad functional group tolerance, excellent enantioselectivities (up to 98.5:1.5 e.r.) and a mild reaction condition, releasing CO_2 as the single by-product. More significantly, the resulting unique enantioenriched 19-membered macrocycle **2f** was found to demonstrate a potent *in vitro* anti-Zika virus (ZIKV) activity without obvious cytotoxicity. Further investigation revealed that the anti-ZIKV activity is presumably attributed to an autophagy inhibition in the early stage of viral infection by down-regulating the expression of autophagy related gene Atg12.

Macrocycles widely exist in natural products, biologically active compounds and marketed drugs, and macrocyclic compounds have their advantages, such as the ability to selectively bind to undruggable targets, improved metabolic stability and passive membrane permeability [1–7]. Among them, macrocycles bearing an enantioenriched dihydrobenzofuran scaffold are an important class of compounds and exhibit a wide range of biological activities, such as anti-cancer, antivirus, anti-inflammatory, and antimicrobial (Fig. 1) [8–11]. Despite these valuable functions, the difficulty of resupply and synthesis largely hampers the sustainability, the exploration of the chemical space and the systematic structure-activity relationship investigations. Thus, the development of efficient synthetic strategies to expeditiously access and enrich diverse enantioenriched dihydrobenzofuran-based macrocycles is highly desirable.

So far, several elegant macrocyclizations such as macrolactonization, lactamization, transition-metal-catalyzed cross-coupling reactions, and ring-closing metathesis (RCM) have been developed (Scheme 1a) [12–19]. Despite great progress, the majority of macrocyclizations rely on cyclizations of linear precursors possessing two terminal reactive functional groups. Macrocyclization through a direct C–H activation approach would be very desirable in terms of atom-and step-economy. Recently, several elegant macrocyclizations *via* a transition-metal-catalyzed C–H activation have been developed (Scheme 1b) [20–31]. Despite considerable efforts in this area, all these protocols are non-enantioselective and limited to synthesis of racemic macrocycles. Therefore, the development of enantioselective C–H macrocyclizations to access enantioenriched macrocycles remain a big challenge but is highly desirable.

* Corresponding authors.
E-mail addresses: yangyaxi@simm.ac.cn (Y. Yang), hhuang@simm.ac.cn (H. Huang), tangwei@simm.ac.cn (W. Tang), zhoubing@simm.ac.cn (B. Zhou).
[1] These authors contributed equally to this work.

https://doi.org/10.1016/j.cclet.2024.109574
1001-8417/

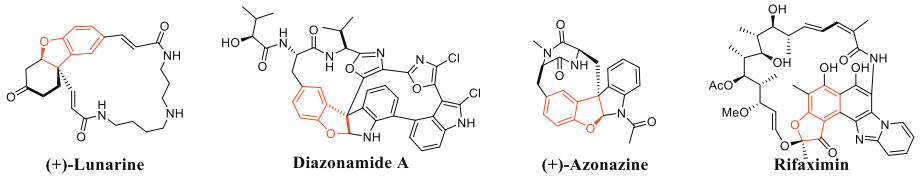

Fig. 1. Representative bioactive macrocycles bearing an enantioenriched dihydrobenzofuran scaffold.

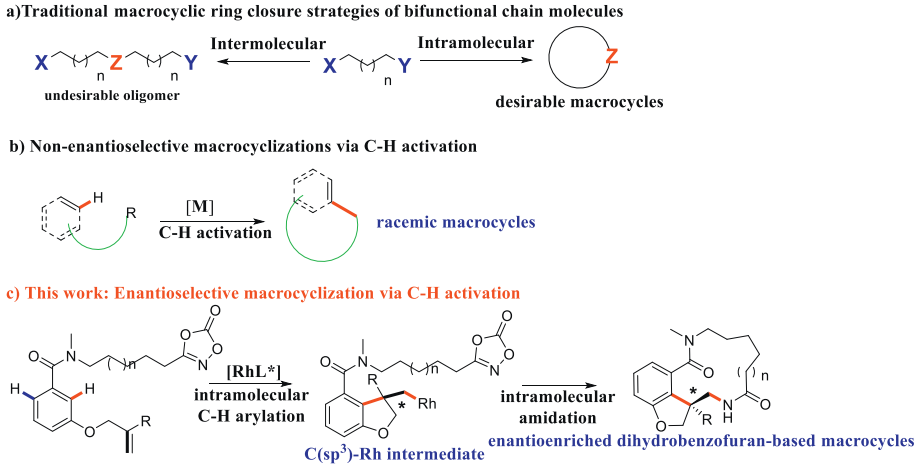

Scheme 1. Synthesis of macrocyclic compounds.

Alkene is an important prochiral functional group and 1,2-difunctionalization of alkenes, especially in a catalytic and enantioselective fashion, is a highly efficient and attractive method, enabling fast increase in molecular complexity and direct access to a series of densely functionalized chiral building blocks from simple starting materials [32–41]. Recently, some elegant examples of transition-metal-catalyzed asymmetric 1,2-difunctionalization of O-tethered-alkenes have been reported to access enantioenriched 2,3-dihydrobenzofurans [42–53]. Stimulated by those pioneering studies and our interest in developing C–H functionalizations [54–56], we envisioned that a "an asymmetric intramolecular 1,2-carboamination of a O-bearing olefin-tethered arenes *via* a C–H activation strategy" strategy could hold promise for a new approach to access structurally diverse enantioenriched dihydrobenzofuran-based macrocycles (Scheme 1c).

However, besides the optimization of the chiral catalysts, there are four challenging issues to be addressed in these scenarios: (a) The intramolecular annulative C–H arylation must be faster than the undesired intramolecular competitive C–H amidation. (b) There are two *ortho* C–H bonds that can be activated. Activation of another undesired C–H bond followed by an intramolecular or intermolecular amidation would provide several undesired byproducts. (c) The C(alkyl)-M intermediate resulting from intramolecular annulative C–H arylation is liable to undergo protonation [44,51]. Thus, the subsequent intramolecular amidation of the C(alkyl)-M intermediate must be faster than protonation. (d) The C(alkyl)-M intermediate can also be trapped through a competitive undesired intermolecular amidation reaction.

Herein, we report the first rhodium(III)-catalyzed enantioselective intramolecular 1,2-carboamidation of aromatic tethered alkenes, enabling the efficient synthesis of structurally diverse enantioenriched dihydrobenzofuran-based macrocycles (Scheme 1c). More significantly, the enantioenriched 19-membered macrocycle **2f** was found to exhibit decent *in vitro* anti-Zika virus (ZIKV) activity without obvious cytotoxicity, which can be attributed to an autophagy inhibition.

To examine the feasibility of this reaction, amide **1a** was chosen as the model substrate. Chiral cyclopentadienyl Rh(III) catalysts have emerged as one of the most powerful catalysts in asymmetric C–H functionalization [57–62] as pioneered by Cramer [60] and Rovis [61]. We first investigated the effect of a famous chiral rhodium catalyst **Rh1** (R = OMe) in the presence of various additives in DCE at 60 °C (Table 1, entries 1–4). The acetate additives were shown to play a critical role to afford the desired macrocyclic product **2a** and $Cu(OAc)_2$ was identified as the superior additive, providing the **2a** in 58% yield (entry 4) with a low enantioselectivity (75:25 e.r.). A further screen of previously reported chiral catalysts **Rh2**–**5** (entries 5–8) revealed that a 3,3′-phenyl substitution was crucial to offer a good enantioselectivity (93:7 e.r.) (entry 8). Considering that the benzene ring of the **Rh5** can form a vertical surface with the BINOL skeleton, we reasonably designed and synthesized a series of new chiral ligands with further substitution on the phenyl ring (**Rh6**, **Rh7** and **Rh8**) (entries 9–11). The novel catalyst **Rh8** provided the best enantioselectivity (98:2 e.r.) also with an accepted yield of 68% at 60 °C (entries 11–13). This macrocyclization reaction does not proceed in 1,4-dioxane, toluene and CH_3CN.

Under the optimal reaction conditions, the substrate scope was investigated (Scheme 2). This reaction could allow to access even larger 15- to 20-membered macrocycles (**2b**–**g**) with good yields and excellent enantioselectivities (up to 98:2 e.r.). The reaction of substrate **1a** bearing various electron-donating or electron-withdrawing substituents at *para* or *meta* position of the arene ring proceeded smoothly, affording compounds **2h**–**p** with good yields and excellent enantioselectivities (97:3–98.5:1.5 e.r.). The absolute configuration of the product **2p** was established by X-ray crystallographic analysis (CCDC: 2059282). When 2-naphthalenecarboxamide was used, the corresponding product **2q** was generated in good yield with excellent enantiomeric ratios (98:2 e.r.). Various substituted allyl groups such as ethyl, bulky cyclopentyl, phenyl, and phenoxymethyl groups also afford the corresponding product (**2r**–**u**) with excellent enantioselectivities (up to 98:2 e.r.).

Table 1
Optimization of reaction conditions.[a]

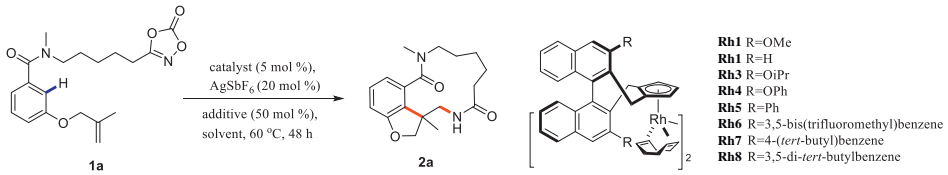

Entry	Catalyst	Additive	Solvent	Yield (%)	e.r.
1	**Rh1**	Ag_2CO_3	DCE	0	/
2	**Rh1**	$Zn(OAc)_2$	DCE	23	74:26
3	**Rh1**	AgOAc	DCE	30	75:25
4	**Rh1**	$Cu(OAc)_2$	DCE	58	75:25
5	**Rh2**	$Cu(OAc)_2$	DCE	38	67:33
6	**Rh3**	$Cu(OAc)_2$	DCE	40	65:35
7	**Rh4**	$Cu(OAc)_2$	DCE	44	75:25
8	**Rh5**	$Cu(OAc)_2$	DCE	50	93:7
9	**Rh6**	$Cu(OAc)_2$	DCE	55	94.5:5.5
10	**Rh7**	$Cu(OAc)_2$	DCE	45	90.5:9.5
11	**Rh8**	$Cu(OAc)_2$	DCE	68	98:2
12[b]	**Rh8**	$Cu(OAc)_2$	DCE	50	98.5:1.5
13[c]	**Rh8**	$Cu(OAc)_2$	DCE	61	96.5:3.5

Conditions:
[a] **1a** (0.1 mmol), catalyst (5 mol%), $AgSbF_6$ (20 mol%) and additive (50 mol%) in solvent (1 mL) at 60 °C for 48 h. Yield isolated by column chromatography and e.r. determined by chiral HPLC.
[b] Reaction was performed at 50 °C.
[c] Reaction was performed at 70 °C.

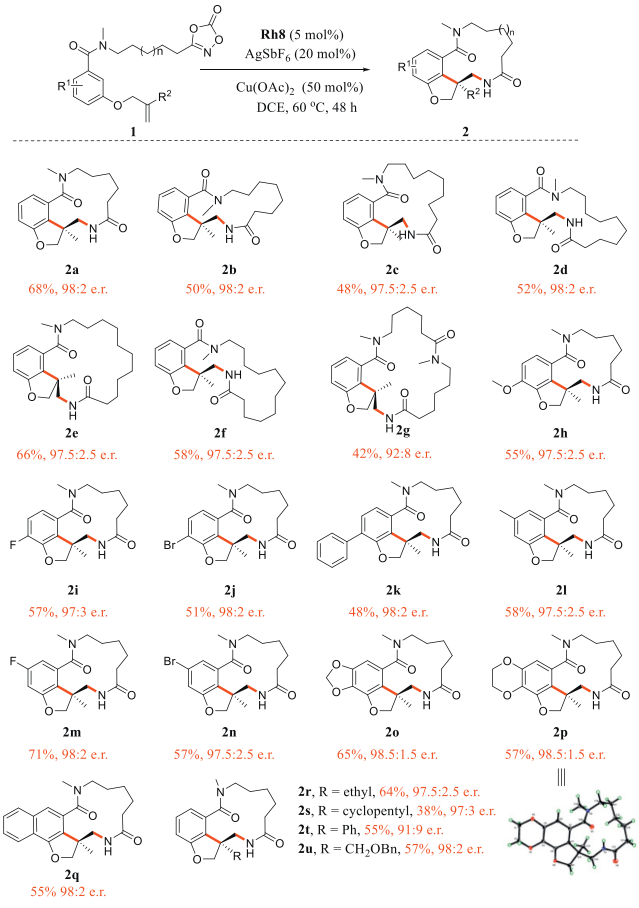

Scheme 2. Substrate scope. Conditions: **1** (0.1 mmol), **Rh8** (5 mol%), $AgSbF_6$ (20 mol%), $Cu(OAc)_2$ (50 mol%) in DCE (1 mL) at 60 °C for 48 h. Isolated yield. The enantiomeric ratio (e.r.) of the products were determined by chiral HPLC in comparison with the authentic racemate.

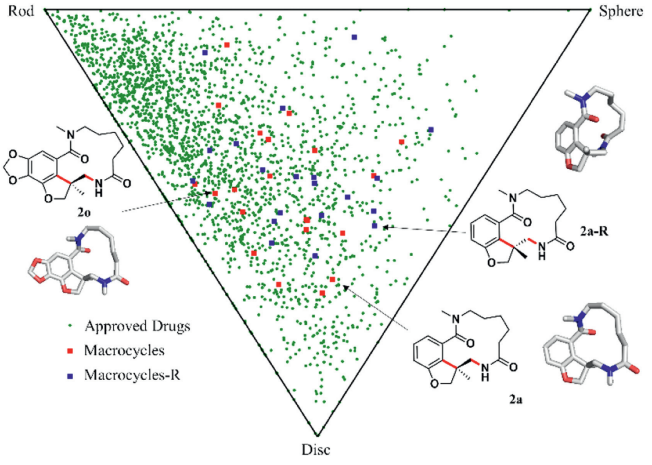

Fig. 2. The molecular shape diversity of the macrocyclic library.

To evaluate the degree of the overall structural diversity of our macrocyclic library, we compared these macrocycles with approved market drugs: (1) 21 synthesized macrocycles, (2) 21 macrocycles with opposite configuration, and (3) 2388 known drugs. Based on the calculations of the lowest energy conformations of these compounds, normalized ratios of principal moment-of-inactiveia (PMI) molecular shape descriptors were drawn on a two-dimensional triangular graph [63]. As shown in Fig. 2, all of the compounds were classified as rods, discs, and spheres to characterize the shape and the distribution of this library around the triangle exhibited the molecular structural diversity. The result demonstrated that most of approved drugs are either disklike or rodlike [64], while these macrocyclic compounds show a considerably higher number of dislike and spherical molecules that are rare in conventional compound libraries, highlighting the advantage of this synthetic method in terms of product diversity.

ZIKV is an emerging flavivirus that causes microcephaly and other severe brain injury in fetuses during pregnancy and also causes neuroinflammatory Guillain-Barré syndrome, neuropathy

and myelitis in adults [65]. In 2016, ZIKV outbreak was declared as a public health emergency of international concern by the World Health Organization (WHO), and over 2 billion people were threatened by ZIKV infection globally [66]. Despite a huge threaten, there are currently no approved treatments or vaccines for ZIKV [67]. Therefore, there is an urgent need for the development of anti-ZIKV drug.

Applying the above method, we created a screening library of various macrocycles and these macrocycles were further evaluated by using various phenotypic assays, including a cytopathic protection assay to investigate the anti-ZIKV activity. To our delight, the results revealed that 19-memebered macrocycle **2f** exhibited a decent cytopathic protection of ZIKV infection in Vero (African green monkey kidney) cell and the ring size of macrocycles is crucial to the inhibitory effect (Table S1 in Supporting information).

Encouraged by the preliminary results, the antiviral activity and mechanism of compound **2f** were further investigated. First, macrocycle **2f** showed no cytotoxicity at the concentration up to 50 μmol/L after 24 h treatment (Fig. 3A). To further evaluate the antiviral activity of **2f**, we next examined the inhibition of ZIKV infection in Vero cells with multiplicity of infection (MOI) = 1 under the treatment of **2f** for 24 h. Intracellular viral RNA levels, viral protein expression levels and virus progeny in supernatants were determined by quantitative real-time PCR polymerase chain reaction (qRT-PCR), Western blot and plaque assay respectively. Compound **2f** decreased viral RNA expression with 50% effective concentration (EC_{50}) of 20.67 μmol/L (Fig. 3B). The genome of ZIKV encodes 10 genes that are translated into three structural proteins (C, prM, and E) and seven non-structural proteins (NS1, NS2A, NS2B, NS3, NS4A, NS4B, and NS5). The real-time PCR revealed that **2f** decreased ZIKV NS1 gene (Fig. 3C) and Western blot showed that **2f** decreased ZIKV NS1 and NS3 protein expression (Figs. 3D and E). Meanwhile, Plaque assay directly reflected the reduction of progeny yield by **2f** treatment (Figs. 3F and G). More importantly, these results showed that **2f** was more potent than ribavirin, a broad-spectrum antiviral drug that has good anti-ZIKV activity and suppresses viremia in ZIKV-infected signal transducer and activator of transcription 1 (STAT1)-deficient mice [68]. Immunofluorescence assay also showed that **2f** inhibited anti-flavivirus group antigen (4G2) expression in a dose-dependent manner (Fig. 3H). Collectively, our data clearly demonstrated that **2f** inhibited ZIKV infection presented by the reduced production of viral RNA and viral protein and the decreased virion yield *in vitro*.

To further explore the underlying mechanism of the inhibitory action of **2f** on ZIKV infection, we performed a quantitative comparison for the Vero cells treated and untreated with compound **2f** by a high-sensitivity label-free quantitative proteomics mass spectrometry approach. In this study, four biological replicates were conducted for each group (control and treat) to ensure the reliability of the results (Figs. S1A and B in Supporting information). The results showed that a total of 8879 proteins were preliminary monitored, among which 8513 proteins with quantitative information were identified. Interestingly, the expression of protein p62 (SQSTM1), an important selective autophagy receptor, increased by 134% with a *P*-value of 2.28E-7 in response to **2f** treatment (Fig. S1C in Supporting information). The deposition of p62 has been widely utilized as a marker for autophagy inhibition or abnormalities in autophagic degradation [69], suggesting that the stimulation

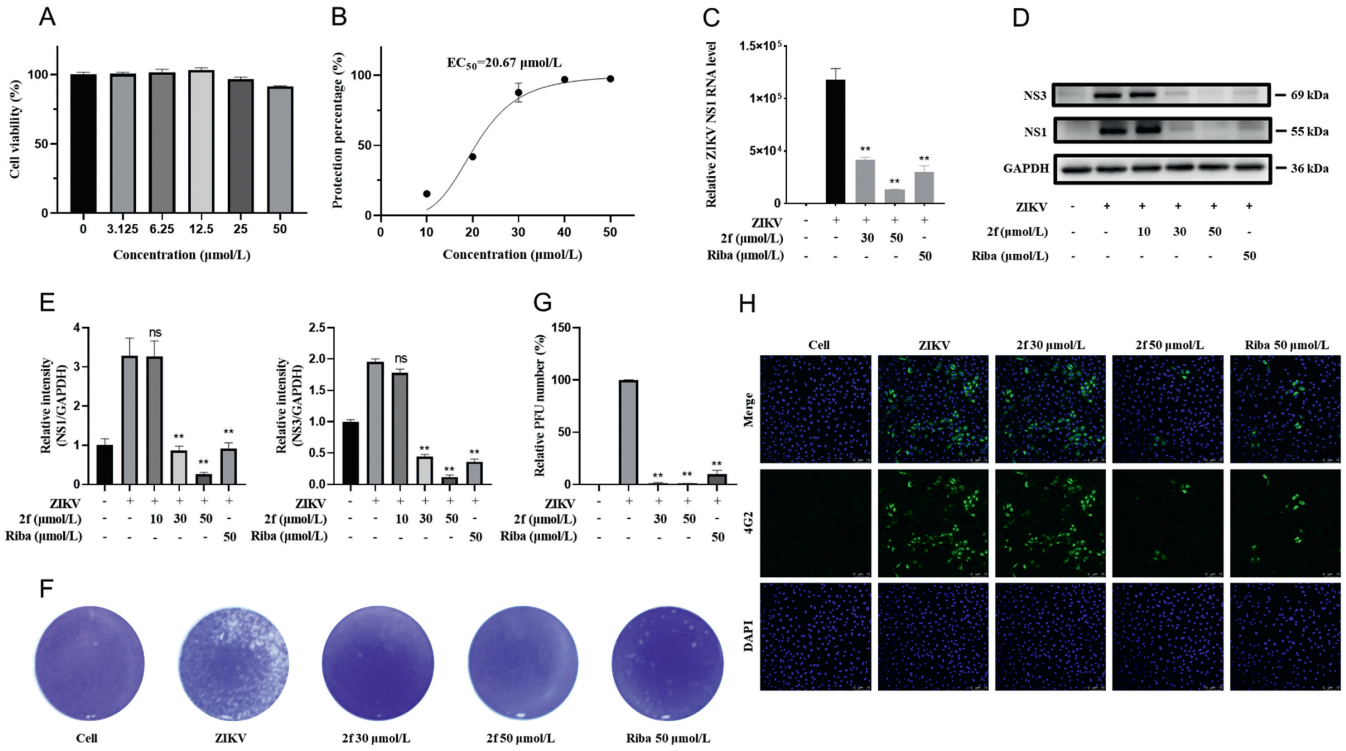

Fig. 3. **2f** Inhibits ZIKV infection in Vero cells. (A) Cytotoxicity of **2f** in Vero cells. Vero cells were treated with different concentrations of **2f** for 24 h, and viability was determined by cell counting kit-8 (CCK8) assays. (B) Antiviral activity of the **2f** against ZIKV. Vero cells were treated with **2f** at different concentrations and were infected with ZIKV at an MOI = 1. The anti-ZIKV activity of **2f** was quantified by qRT-PCR with a primer designed for the NS1 gene. Percentage (%) were calculated as the **2f** treatment viral genome load *vs.* the virus control. (C) Viral RNA was measured by qRT-PCR with a positive control ribavirin (Riba) at 50 μmol/L as well. (D) Western blot analyzed the expression of ZIKV-NS1, ZIKV-NS3 after infection for 24 h with or without **2f**. (E) Image analysis and quantitation for Western blot by using ImageJ software. (F) ZIKV titers from cell supernatants were determined by infecting Vero cells for 4 days with an agarose overlay and the plate was photographed. The plates were analyzed for plaque-forming units per mL (PFU/mL). (G) Virus yield was assessed by plaque-forming unit assay. (H) Immunofluorescent staining for 4G2 in Vero cells. Scale bar: 75 μm. Data are shown as the (means ± SD) of three independent experiments. Statistical significance was analyzed from one-way-ANOVA compared with the ZIKV group. $^{**}P < 0.01$ *vs.* the virus control. GAPDH, glyceraldehyde-3-phosphate dehydrogenase; DAPI, 4′,6-diamidino-2-phenylindole; ns, no significance.

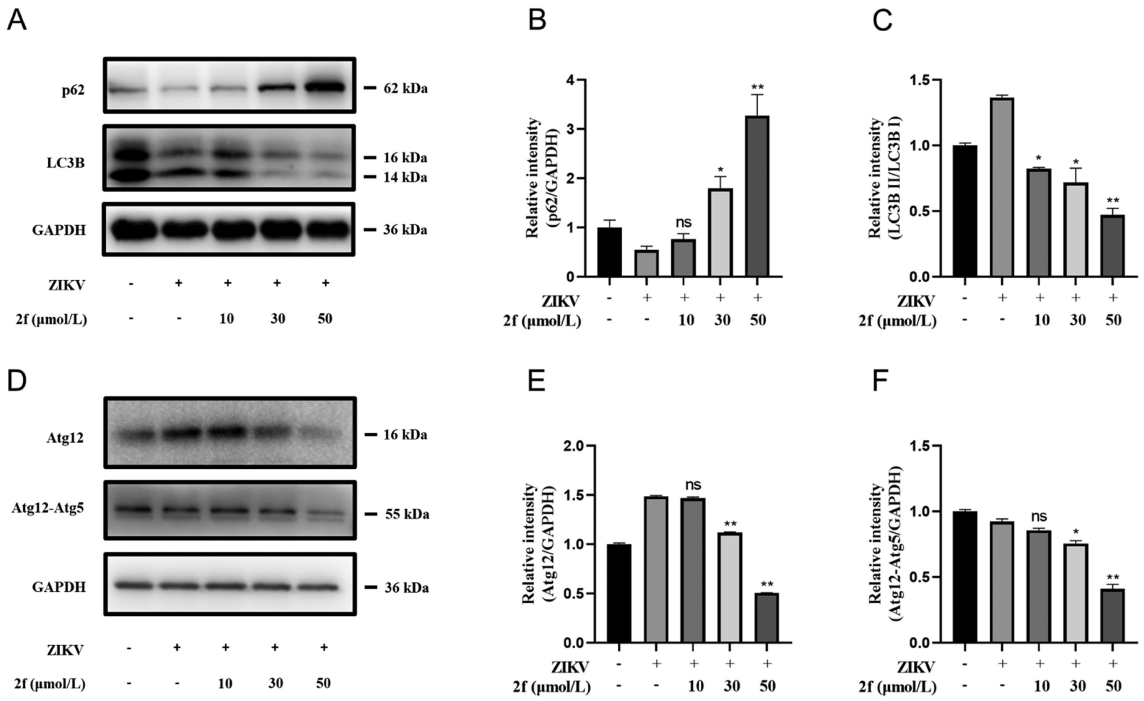

Fig. 4. **2f** Suppresses autophagy by reducing Atg12 expression. (A) Western blot analysis of p62 and LC3B expression levels in Vero cells infected with ZIKV and treated with **2f**. (B, C) Quantification results of p62 protein expression, LC3B-II:I ratio levels ($n = 3$ independent experiments). (D) Western blot analysis of Atg12, Atg12–Atg5 complex protein expression levels in Vero cells infected with ZIKV and treated with **2f**. (E, F) Quantification results of Atg12 protein expression, Atg12–Atg5 levels ($n = 3$ independent experiments). Data are shown as the means ± SD of three independent experiments. Statistical significance was analyzed from one-way-ANOVA compared with the ZIKV group, $^{*}P < 0.05$, $^{**}P < 0.01$ *vs.* the virus control.

from compound **2f** could influence the physiological processes involved in autophagy.

Autophagy, which is involved in the degradation and recycling of cellular components, was reported to promote the replication of ZIKV and dengue virus [70–72]. In autophagy, cytoplasmic components are engulfed by autophagosomes and delivered to lysosomes for degradation. Microtubule-associated proteins light chain 3 (LC3) is considered as indicators of autophagy when LC3 I converses to LC3 II [73]. Encouraged by the above findings, we further detected LC3 II/I and p62 protein involved in autophagy. As shown in Figs. 4A–C, LC3 II level was decreased and autophagy substrates p62 expression level was increased with the treatment of **2f** in a dose-dependent manner, indicating that the cell autophagy was inhibited. The Atg12 ubiquitin-like binding system plays an important role in the formation of autophagosomes. It has also been shown that the complex may contribute to the initial tethering of vesicle precursors during autophagosome formation. To examine whether **2f** affects the activity of Atg5–Atg12 complex to inhibit the autophagy process, we examined the protein expression level of the Atg5–Atg12 complex and its monomers (Figs. 4D–F). The results showed that **2f** significantly down-regulated the protein expression level of Atg5–Atg12 complex and its monomer, especially for Atg12. Taken together, these results demonstrated that during the infection of ZIKV in Vero cells, **2f** inhibited the lipidation of LC3 by down-regulating the expression of Atg12, preventing the process of autophagy and inhibiting the replication of the ZIKV on Vero cell.

In summary, we have demonstrated for the first time that an enantioselective intramolecular 1,2-carboamidation of alkenes is a feasible enantioselective macrocyclization leading to enantioenriched macrocycles. This robust asymmetric C–H macrocyclization proceeds with a broad functional group tolerance under mild reaction conditions, affording structurally diverse dihydrobenzofuran-based macrocycles with excellent enantioselectivity (up to 98.5:1.5 e.r.). The synthesized compounds were more dislike and spherical in shape than previous macrocyclic drugs, thus expanding the chemical space of macrocycles. More significantly, the unique enantioenriched 19-memebered macrocycle **2f** was found to potently inhibit ZIKV infection in Vero cells without obvious cytotoxicity. Further mechanism investigation revealed that **2f** could inhibit the occurrence of autophagy in the early stage of viral infection by down-regulating the expression of autophagy related gene Atg12, which provides a new idea and experimental basis for anti-ZIKV drug development.

Declaration of competing interest

The authors declare that they have no known competing financial interests or personal relationships that could have appeared to influence the work reported in this paper.

Acknowledgments

This work was supported by National Natural Science Foundation of China (No. 81973166), Science and Technology Commission of Shanghai Municipality (No. 22XD1424600), Natural Science Foundation of Shanghai Municipality (No. 22ZR1474100), Taishan Scholar Foundation of Shandong Province (No. tsqn202306322), National Key R&D Program of China (No. 2021YFC2300700), Shandong Laboratory Program (No. SYS202205), Shandong Provincial Natural Science Foundation (Nos. ZR2023LSW003 and ZR2023JQ028).

Supplementary materials

Supplementary material associated with this article can be found, in the online version, at doi:10.1016/j.cclet.2024.109574.

References

[1] E.M. Driggers, S.P. Hale, J. Lee, N.K. Terrett, Nat. Rev. Drug Discov. 7 (2008) 608–624.
[2] E.A. Crane, K.A. Scheidt, Angew. Chem. Int. Ed. 49 (2010) 8316–8326.
[3] J. Mallinson, I. Collins, Future Med. Chem. 4 (2012) 1409–1438.
[4] D.J. Newman, G.M. Cragg, Bioactive macrocycles from nature, in: J. Levin (Ed.), Macrocycles in Drug Discovery, Royal Soc. Chem., Cambridge, 2015, pp. 1–36.
[5] E. Marsault, M.L. Peterson, J. Med. Chem. 54 (2011) 1961–2004.
[6] P. Ermert, Chimia 71 (2017) 678–702.
[7] H. Itoh, M. Inoue, Chem. Rev. 119 (2019) 10002–10031.
[8] C.J. Hamilton, A. Saravanamuthu, C. Poupat, A.H. Fairlamb, I.M. Eggleston, Bioorg. Med. Chem. 14 (2006) 2266–2278.
[9] N. Lindquist, W. Fenical, G.D. Van Duyne, J. Clardy, J. Am. Chem. Soc. 113 (1991) 2303–2304.
[10] Q.X. Wu, M.S. Crews, M. Draskovic, et al., Org. Lett. 12 (2010) 4458–4461.
[11] J.C. Gillis, R.N. Brogden, Rifaximin. Drugs 49 (1995) 467–484.
[12] R.H. Grubbs, S.J. Miller, G.C. Fu, Acc. Chem. Res. 28 (1995) 446–452.
[13] G.S.C. Srikanth, S.L. Castle, Tetrahedron 61 (2005) 10377–10441.
[14] A. Gradillas, J. Pérez-Castells, Angew. Chem. Int. Ed. 45 (2006) 6086–6101.
[15] A.H. Hoveyda, A.R. Zhugralin, Nature 450 (2007) 243–251.
[16] A. Parenty, X. Moreau, G. Niel, J.M. Campagne, Chem. Rev. 113 (2013) PR1–PR40.
[17] Y. Li, X. Yin, M. Dai, Nat. Prod. Rep. 34 (2017) 1185–1192.
[18] C.A.G.N. Montalbetti, V. Falque, Tetrahedron 61 (2005) 10827–10852.
[19] R. Peng, Y. Xu, Q. Cao, Chin. Chem. Lett. 29 (2018) 1465–1474.
[20] K.J. Fraunhoffer, P. Narayanasamy, L.E. Sirois, M.C. White, J. Am. Chem. Soc. 128 (2006) 9032–9033.
[21] E.M. Stang, M.C. White, Nat. Chem. 1 (2009) 547–551.
[22] E.M. Stang, M.C. White, Angew. Chem. Int. Ed. 50 (2011) 2094–2097.
[23] J.P. Krieger, G. Ricci, D. Lesuisse, C. Meyer, J. Cossy, Eur. J. Org. Chem. 22 (2016) 13469–13473.
[24] H. Kim, S. Chang, Angew. Chem. Int. Ed. 56 (2017) 3344–3348.
[25] A. Lumbroso, N. Abermil, B. Breit, Chem. Sci. 3 (2012) 789–793.
[26] M.P. Doyle, M.N. Protopopova, C.D. Poulter, D.H. Rogers, J. Am. Chem. Soc. 117 (1995) 7281–7282.
[27] W. Liu, Z. Ren, A.T. Bosse, et al., J. Am. Chem. Soc. 140 (2018) 12247–12255.
[28] B. Jiang, M. Zhao, S.S. Li, Y.H. Xu, T.P. Loh, Angew. Chem. Int. Ed. 57 (2018) 555–559.
[29] X. Lu, S.J. He, W.M. Cheng, J. Shi, Chin. Chem. Lett. 29 (2018) 1001–1008.
[30] T. Bi, Y. Xu, X. Xu, et al., Chin. Chem. Lett. 33 (2022) 2015–2020.
[31] S. Hu, Y. Zhang, X. Xie, et al., Chin. Chem. Lett. 35 (2024) 109408.
[32] W. Zeng, S.R. Chemler, J. Am. Chem. Soc. 129 (2007) 12948–12949.
[33] D.N. Mai, J.P. Wolfe, J. Am. Chem. Soc. 132 (2010) 12157–12159.
[34] B.A. Hopkins, J.P. Wolfe, Angew. Chem. Int. Ed. 51 (2012) 9886–9890.
[35] T. Piou, T. Rovis, Nature 527 (2015) 86–90.
[36] D.R. White, J.T. Hutt, J.P. Wolfe, J. Am. Chem. Soc. 137 (2015) 11246–11249.
[37] V. Bizet, G.M. Borrajo-Calleja, C. Besnard, C. Mazet, ACS Catal. 6 (2016) 7183–7187.
[38] Z. Liu, Y. Wang, Z. Wang, et al., J. Am. Chem. Soc. 139 (2017) 11261–11270.
[39] D.S. Brandes, A. Sirvent, B.Q. Mercado, J.A. Ellman, Org. Lett. 23 (2021) 2836–2840.
[40] K. Ozols, S. Onodera, Ł. Woźniak, N. Cramer, Angew. Chem. Int. Ed. 60 (2021) 655–659.
[41] S. Maity, T.J. Potter, J.A. Ellman, Nat. Catal. 2 (2019) 756–762.
[42] S.G. Newman, J.K. Howell, N. Nicolaus, M. Lautens, J. Am. Chem. Soc. 133 (2011) 14916–14919.
[43] H. Cong, G.C. Fu, J. Am. Chem. Soc. 136 (2014) 3788–3791.
[44] B. Ye, P.A. Donets, N. Cramer, Angew. Chem. Int. Ed. 53 (2014) 507–511.
[45] W. You, M.K. Brown, J. Am. Chem. Soc. 137 (2015) 14578–14581.
[46] Z.M. Zhang, B. Xu, Y. Qian, et al., Angew. Chem. Int. Ed. 57 (2018) 10373–10377.
[47] Z.M. Zhang, B. Xu, L. Wu, et al., J. Am. Chem. Soc. 141 (2019) 8110–8115.
[48] R.C. Carmona, O.D. Köster, C.R.D. Correia, Angew. Chem. Int. Ed. 57 (2018) 12067–12070.
[49] Z.X. Tian, J.B. Qiao, G.L. Xu, et al., J. Am. Chem. Soc. 141 (2019) 7637–7643.
[50] Z.M. Zhang, B. Xu, L. Wu, et al., Angew. Chem. Int. Ed. 58 (2019) 14653–14659.
[51] G. Li, Q. Liu, L. Vasamsetty, W. Guo, J. Wang, Angew. Chem. Int. Ed. 59 (2020) 3475–3479.
[52] J. He, Y. Xue, B. Han, et al., Angew. Chem. Int. Ed. 59 (2020) 2328–2332.
[53] W. Yu, C. Chen, L. Feng, et al., Org. Lett. 24 (2022) 1762–1767.
[54] Y. Wu, Z. Chen, Y. Yang, W. Zhu, B. Zhou, J. Am. Chem. Soc. 140 (2018) 42–45.
[55] B. Zhou, Z. Chen, Y. Yang, et al., Angew. Chem. Int. Ed. 54 (2015) 12121–12126.
[56] Y. Yang, X. Wang, Y. Li, B. Zhou, Angew. Chem. Int. Ed. 54 (2015) 15400–15404.
[57] B. Ye, N. Cramer, Acc. Chem. Res. 48 (2015) 1308–1318.
[58] C.G. Newton, D. Kossler, N. Cramer, J. Am. Chem. Soc. 138 (2016) 3935–3941.
[59] C.G. Newton, S.G. Wang, C.C. Oliveira, N. Cramer, Chem. Rev. 117 (2017) 8908–8976.
[60] B. Ye, N. Cramer, Science 338 (2012) 504–506.
[61] T.K. Hyster, L. Knörr, T.R. Ward, T. Rovis, Science 338 (2012) 500–503.
[62] S. Satake, T. Kurihara, K. Nishikawa, et al., Nat. Catal. 1 (2018) 585–591.
[63] W.H.B. Sauer, M.K. Schwarz, J. Chem. Inf. Comput. Sci. 43 (2003) 987–1003.
[64] T. Yang, Z. Li, Y. Chen, et al., Nucleic Acids Res. 49 (2021) D1170–D1178.
[65] C. Li, D. Xu, Q. Ye, et al., Cell Stem Cell 19 (2016) 120–126.
[66] J.P. Messina, M.U. Kraemer, O.J. Brady, et al., eLife 5 (2016) e15272.
[67] J.A. Bernatchez, L.T. Tran, J. Li, et al., J. Med. Chem. 63 (2020) 470–489.
[68] N. Kamiyama, R. Soma, S. Hidano, Antiviral Res. 146 (2017) 1–11.
[69] G. Bjørkøy, T. Lamark, A. Brech, et al., J. Cell Biol. 171 (2005) 603–614.
[70] R. Hamel, O. Dejarnac, S. Wichit, et al., J. Virol. 89 (2015) 8880–8896.
[71] Q. Liang, Z. Luo, J. Zeng, et al., Cell Stem Cell 19 (2016) 663–671.
[72] Y.R. Lee, H.Y. Lei, M.T. Liu, et al., Virology 374 (2008) 240–248.
[73] Y. Kabeya, N. Mizushima, A. Yamamoto, et al., J. Cell Sci. 117 (2004) 2805–2812.